LAPPEENRANTA UNIVERSITY OF TECHNOLOGY
DEPARTMENT OF ELECTRICAL ENGINEERING

Oxygen adsorption on Cu(211) and structurally and chemically modified Cu(100)

The supervisor of this study was Professor Matti Alatalo and the examiner was M.Sc. Antti Puisto.

Helsinki 14.9.2007

Nelli Nivalainen
Näyttelijäntie 24 e 59
00400 Helsinki
Tel. +358-50-5470023

Abstract

Author: Nivalainen, Nelli Johanna

Subject: **Oxygen adsorption on Cu(211) and structurally and chemically modified Cu(100)**

Department: Department of Electrical Engineering

Year: 2007

Lappeenranta University of Technology, Master's Thesis, 52 pages, 43 figures and 7 tables.

Supervisor: Professor Matti Alatalo

Examiner: M.sc. Antti Puisto

Keywords: Copper, Silver, Oxygen, Adsorption, Oxidation

Oxidation of copper has recently been under broad interest among material scientists as copper is a widely used material in manufacturing industry and the developing of applications, such as protective surface oxides, is possible only with thorough knowledge of oxidation process. Under normal circumstances metals include different kinds of lattice defects, so also their effects on the oxidation process should be known well. This thesis concentrates thus on mechanisms through which defects and steps affect on a copper surface.

This study has been made by using calculational methods and VASP and SIESTA simulation programs. In the study Cu(100) surface is used for studying chemical and structural defects as it is the most reactive low Miller's index surface and Cu(211) is used for step surface calculations, as it is a simple, stable and widely studied surface structure.

As structural defects, adatoms have an inhibitive impact on dissociation, but in contrast, vacancies act as dissociative centres. Doping copper with silver, which was used as chemical impurity, doesn't prevent oxidation as an interesting segregation phenomenon occurs during the oxidation process and silver gets pushed towards the bulk. In the case of a step surface Cu(211), hollow site on (100) microfacet was found to be the most dissociative site and bridge site on the step edge the most suitable site for molecular adsorption. A copper step (211) surface was also found to be more reactive than the smooth copper surfaces.

Tiivistelmä

Tekijä:	Nivalainen, Nelli Johanna
Nimi:	**Oxygen adsorption on Cu(211) and structurally and chemically modified Cu(100)**
Osasto:	Sähkötekniikan osasto
Vuosi:	2007

Lappeenrannan teknillinen yliopisto, Diplomityö, 52 sivua, 43 kuvaa ja 7 taulukkoa.

Ohjaaja:	Professori Matti Alatalo
Tarkastaja:	DI Antti Puisto
Hakusanat:	Kupari, Hopea, Happi, Adsorptio, Hapettuminen

Kuparipinnan hapettuminen on viimevuosina ollut suosittu tutkimuskohde materiaalitieteissä kuparin laajan teollisuuskäytön vuoksi. Teollisuussovellusten, kuten suojaavien pintaoksidien kehittäminen vaatii kuitenkin syvällistä tuntemusta hapettumisprosessista ja toisaalta myös normaaliolosuhteissa materiaalissa esiintyvien hilavirheiden vaikutuksesta siihen. Tässä työssä keskitytäänkin tutkimaan juuri niitä mekanismeja, joilla erilaiset pintavirheet ja porrastettu pintarakenne vaikuttavat hapen adsorptioprosessiin kuparipinnalla.

Tutkimus on tehty käyttämällä laskennallisia menetelmiä sekä VASP- ja SIESTA-ohjelmistoja. Työssä tutkittiin kemiallisia ja rakenteellisia virheitä Cu(100)-pinnalla, joka on reaktiivisin matalan Millerin indeksin pinta ja porrastetun pinnan tutkimuksessa käytettiin Cu(211)-pintaa, joka puolestaan on yksinkertainen, stabiili ja aiemmissa tutkimuksissa usein käytetty pintarakenne.

Työssä tutkitut hilavirheet, adatomit, vähentävät molekyylin dissosiaatiota kuparipinnalla, kun taas vakanssit toimivat dissosiaation keskuksina. Kemiallisena epäpuhtautena käytetty hopeakerros ei estä kuparin hapettumista, sillä happi aiheuttaa mielenkiintoisen segregaatioilmiön, jossa hopea työntyy syvemmälle pinnassa jättäen kuparipinnan suojaamattomaksi. Porrastetulla pinnalla (100)-hollow on todennäköisin paikka molekyylin dissosiaatiolle, kun taas portaan bridge-paikka on suotuisin molekulaariselle adsorptiolle. Lisäksi kuparin steppipinnan todettiin olevan reaktiivisempi kuin tasaiset kuparipinnat.

Preface

This thesis was written for the Department of Electrical Engineering at Lappeenranta University of Technology and it is a part of the Surfox-project organized by Tekes.

I would like to acknowledge my supervisor, Professor Matti Alatalo, for his help, advisory and support as well as my instructor, M. sc. Antti Puisto, for his help and guidance during this project. Many thanks also to other members of the laboratory.

I would also like to thank all my friends for making the years in Lappeenranta so great. Special thanks to Joni for being there for me and cheering me up when needed. Last but not least, I want to thank my family, especially my parents, for enormous support during my studies.

Contents

Abbreviations

APW	Augmented Plane Wave
DFT	Density Functional Theory
DOS	Density of States
GGA	Generalized Gradient Approximation
LCAO	Linear Combination of Atomic Orbitals
LDA	Local Density Approximation
MD	Molecular Dynamics
NCPP	Norm-conserving pseudopotential
PAW	Projector Augmented Waves
PES	Potential Energy Surface
PW	Plane-Wave
SIESTA	Spanish Initiative for Electronic Simulations with Thousands of Atoms
SPALEED	Spot Profile Analysis Low Energy Electron Diffraction
US-PP	Ultrasoft Pseudopotential
VASP	Vienna ab-initio simulation package

1 Introduction

From the industrial point of view oxidation is one of the most important reactions when concerning metal surfaces. Motivation for studying copper is due to its popularity in manufacturing and results can give us also information about oxidation of transition metals. In order to prevent unwanted corrosion of metals it is important to understand oxidation phenomena thoroughly. Knowledge about controlled oxidation can be used for example in the developement of new catalysts and protective surface oxides.

In this work we study the adsorption of molecular oxygen on Cu(100) surface, which has been modified by adding lattice defects to the surface. Normally metals have different kinds of lattice defects so it is useful to study how they affect the oxidation phenomenon. In this case adatoms and vacancies are used as point defects. Cu(100) surface was chosen, because it is the most reactive low-index copper surface.

In the second part of the work, atomic adsorption of oxygen on clean and silver doped Cu(100) surfaces is studied in order to find out how silver affects the oxidation phenomena. Using silver as an impurity is also a good example of chemical modifications occured on surfaces and thus worth studying.

In the last part of the work molecular oxidation on copper step surface is studied. Steps are a common feature of metal surfaces and Cu(211) surface was chosen for this part of the study as it represents a(100)$\times$(111) cut the stability which of has been found to be high in the case of Cu and Pd in study made by Kóllar et al [1]. Cu(211) is also a simple and widely studied surface and therefore it is a suitable target for studying the adsorption mechanism on a step surface. Cu(211) surface consists of three-atom (111) terraces separated by single-atom (100) microfacets as can be seen in figure 1. Due to this structure it is interesting to estimate how much a different kind of surrounding structure affects the adsorption of oxygen when comparing the results from calculations on (100) micro facet of Cu(211) and Cu(100) surface [2]. We will also compare the calculations to results obtained for Pd(211) surface [3].

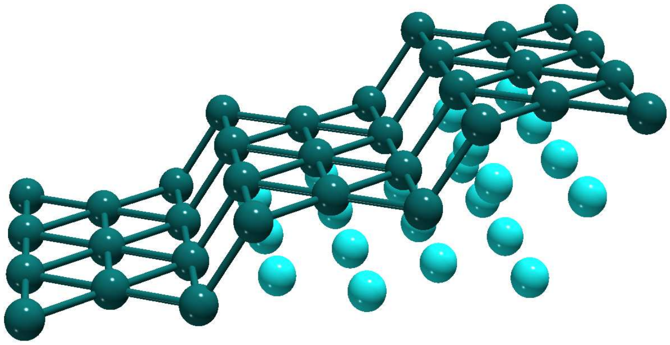

Figure 1: Structure of Cu(211) surface. Figure is rendered by H. Pitkänen.

2 Methods

In this section the programs used in this work are introduced as well as some theory concerning adsorption, density of states and molecular dynamics, which form a central theoretical base for this study.

2.1 Programs: SIESTA and VASP

SIESTA (Spanish Initiative for Electronic Simulations with Thousands of Atoms) is both a method and a computer program developed by J. Soler et al. [4, 5] for accomplishing electronic structure calculations and $ab\ initio$ molecular dynamics simulations. $Ab\ initio$ means that calculation is made from first princples and it relies on basic and proven physical laws without contributory presumptions. When studying chemical reactions both static properties such as geometrical configurations and dynamic properties like diffusion are of interest. These properties can be obtained by calculating the full solution of the many-body Schrödinger equation. Many methods for solving the equation, including the Hartree-Fock theorem were developed, but using of them is limited to calculations with only a small number of active electrons as effort of calculating and storing the wave function depends exponentially on the number of the electrons. [6]

As a solution for this problem, Hohenberg and Kohn proposed the density functional theory (DFT) in 1964, which was first found to be a useful method in solid-state physics where periodic structures are dealt with. SIESTA is based on DFT, which states that the properties of a system can be calculated from the ground state density of the system and thus the calculations are simpler because a simple three-dimensional function of the ground-state density is used instead of the multi-dimensional wave function. Although DFT is an exact theory, it's implementations, like SIESTA, are based on approximations of the exchange-correlation functional.

The SIESTA method uses the linear combination of atomic orbitals (LCAO) [7] and norm conserving pseudopotentials (NCPP) [8, 9] to calculate the groundstate properties of a system. The LCAO approximation is based on the fact that in atoms the electrons are tightly bound to their nuclei and if atoms are close enough their wave functions will overlap. This will happen when atoms are so close that their separations are consistent with the lattice constant. In LCAO the electronic wave functions in the solid are approximated by linear combination of atomic orbitals and the band structure can be defined by a small number of overlap parameters. The overlap parameters simply describe interactions between electrons and neighbouring atoms. [10, 11, 12]

In figure 2 the principle of LCAO is shown. If two overlapping atomic orbitals increase the probability density along the connecting line between the atoms, the atoms have a chemical bond. This state is called bonding molecular state and it can be seen in the top row of the figure. In the top row two atoms have the same signs and in the bottom row they have opposite signs. The latter situation describes an anti-bonding molecular orbital. [13]

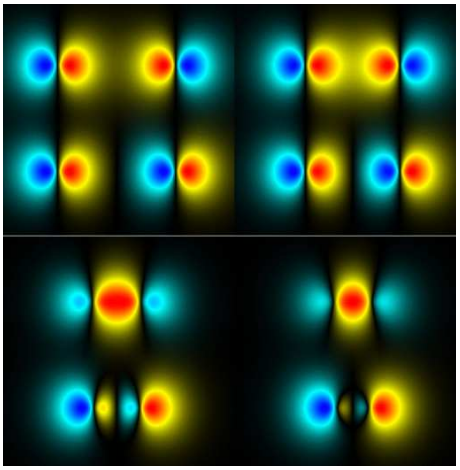

Figure 2: Linear combination of orbitals. The top row describes a bonding molecular state and the bottom row is an anti-bonding molecular state [13].

The difficulty of electronic structure methods is to describe wave functions of a real material because of the differences in various locations of space; close to the nucleus the wave function oscillates rapidly and elsewhere it is quite smooth. Because of the oscillation the calculations of core electrons are time-consuming. Chemical properties of most atoms are determined by their valence electrons and there isn't any important information in the core electrons and therefore a reasonable electronic-structure method may avoid to calculate them. The problem can be solved by using the pseudopotential approximation whose consumption in computer simulation time is one per several hundred compared to all electron potentials, which include all the electrons of the system.

Norm-conserving pseudopotentials, which are used in SIESTA, are made to simplify the application of pseudopotentials and on the other hand make them more accurate and transferable. They were made to fulfill especially the following requirements: pseudopotential should describe the long-range interaction of the core, outside of a core radius the pseudo-wavefunction should agree with the all-electron wavefunction and inside both the pseudopotential and the wavefunction should be as smooth as possible to decrease the computational time. Inspite of good qualities of pseudopotentials, they also make results more inaccurate as happens always when approximations are used. [14, 15]

It should be noted that due to the different basis in calculations, total energies calculated with SIESTA can not be compared with energies obtained from calculations performed with another method. As an example, however, adsorption energies are comparable.

VASP (Vienna Ab-initio Simulation Package) is a program for performing ab-initio quantum-mechanical molecular dynamics simulations using pseudopotentials or the Projector Augmented Waves (PAW) method and a plane wave basis set. The approach executed in VASP is based on the local-density approximation (LDA), which is the most commonly used approximation established by Kohn and Sham [16]. In these calculations, however, Generalized Gradient Approximation (GGA), which can be thought as a modification of LDA, is used.

In this work, the PAW method is used with VASP as an approximation in order to reduce the computer simulation time. Compared to the existing approximation methods PAW is expected to give a similar level of optimization and still be more efficient. DFT forms the basis of PAW and the method includes many properties from the existing linear methods and the pseudopotential method. For example, PAW introduces projectors acting on smooth valence functions and auxiliary localized functions like the ultrasoft pseudopotential method (US-PP) [17]. Localized functions keep all the information on the core states such as the Augmented Plane wave (APW) method. For that reason it can be assumed that PAW is closing the gap between US-PP and APW. [18]

Since PAW is based on DFT, The Schrödinger equation must be solved when a particle system is described by quantum mechanical laws. The Schrödinger equation, which is also called the quantum mechanical wave equation, is a function of both time and place.

In augmented-wave methods the problem of time-consuming calculations of core electrons has been solved by dividing the wave function into parts. In PAW all integrals are calculated as a combination of integrals of smooth functions covering throughout space with localized parts estimated by radial integration over muffin-tin spheres [14]. The muffin-tin potential is an approximation to spherical regions around each nucleus and constant potential in between the spheres. The muffin tin spheres are shown in figure 3

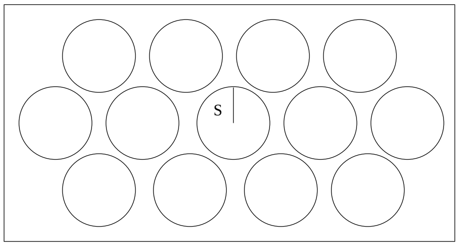

Figure 3: The muffin-tin spheres. The potential is the spherical average of so-called effective potential inside the spheres and constant outside the spheres. The effective potential was defined by Kohn and Sham [16].

2.2 Adsorption

The study of adsorption has a centre stage in the examination of materials. Adsorption is a process that occurs when an adsorbate comes on the surface and forms a molecular or atomic film. Adsorption takes place in different ways, generally classified as physisorption and chemisorption. Physisorption is the weakest form of adsorption and there is no true chemical bond between the surface and adsorbate. Van der Waals force causes the sticking and although it's usually weak, it is important for the bonding in many materials. Contrary to physisorption, in chemisorption true chemical bond is created. There is hybridization between the adsorbate and subrate electronic states which modify the electronic structure.

In this work oxygen adsorption is studied on structured surfaces. The simplest step surfaces are widely studied, because they can be made quite easily in experiment and electronic structure calculations can also be made due to the simplicity of the surfaces. Previous studies (such as [19, 20, 21]) have shown that many adsorbates bind much stronger to the step sites than to the sites on a flat terrace, so the influence of steps can be rather markable also in this case.

When different reactions on surfaces are concerned, there is a couple of simple examples, which are relevant for this study. If a gas molecule such as oxygen hits a surface, it can be reflected or bind to the surface. The binding may happen with molecular or dissociative adsorption and in a few cases molecules can dissociate and only part of the atoms rest on the surface. In figure 4, an illustration of the dissociative adsorption on a surface is shown. [15]

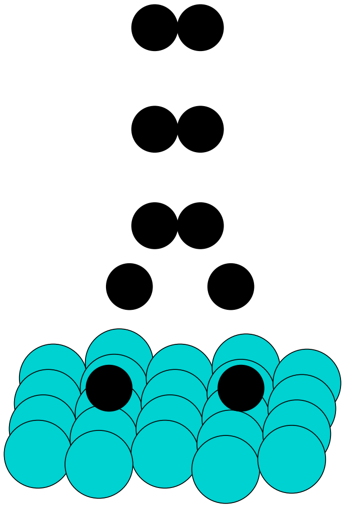

Figure 4: Dissociative adsorption process for a diatomic molecule.

Potential energy surface (PES) of the system has a central role in theoretical describtion of adsorption. PES calculation gives information for instance about adsorption sites and energies and vibrational frequencies of an adsorbate. It also shows if there are barriers for adsorption.

In this work we are using 2-dimensional contour plots of 6-dimensional surfaces, which are called elbow plots due to their shape. For PES plots several total energy calculations are made with varying distances between the atoms of a molecule (i.e. bond lenghts). While the distances were changed, the molecule was also moved towards the surface. Close to the surface dissociative adsorption is energetically more favorable than molecular adsorption as energy is gained upon the adsorption of two distinct atoms. This energy gain upon adsorption is typical for chemisorption. [15]

As it was mentioned in a previous study [22], static PES calculations do not consider the dynamics of a surface. On the other hand, in a finite temperature molecule has kinetic energy, which is neither considered in the PES calculations. These facts led us to use also molecular dynamics simulations for the interesting situations that the PES calculations had revealed. A phenomenon called steering effect is also related to this problem with PES calculations. At low kinetic energies the molecules are so slow, that they can be efficiently steered to a favorable configuration for dissociation, which leads to a high dissociation probability. For example M. Alatalo et al. have found this phenomenon on Cu(100) surface in a recently published study [2]. If the molecule has only a small, for example 0,01 eV kinetic energy and unfavorable configuration for dissociative adsorption, the forces acting upon the molecule can still steer it towards the more favorable sites. When the kinetic energy is higher, the molecule is too fast and can thus scatter back into gas-phase which decreases the probability of sticking. This phenomenon is shown in figure 5 where the kinetic energy of the molecule is 0.12 eV. At even higher kinetic energy, the molecule has enough energy to enter the dissociation channel over the barrier and the sticking probability increases again. [23]

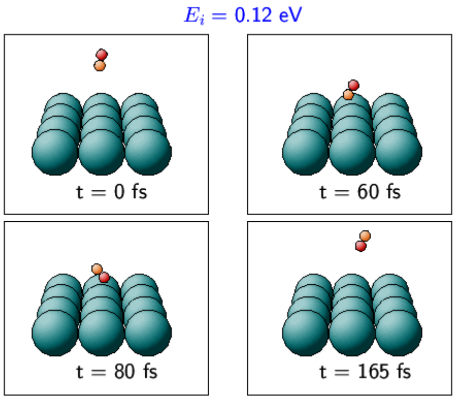

Figure 5: A classical trajectory run with a molecule which is scattering back to the gas phase when the kinetig energy is 0.12 eV. [23]

2.3 Density of States

Density of states (DOS) tells about the interaction between for example the adsorbate and subtrate. The total density of states includes all electrons of the system. In a bond breaking - bond formation process one is usually interested in what happens to the electronic orbitals of the directly involved orbitals of the molecule and the substrate. Usually the information is easier to identify in the local partial density of states, which means that the DOS is divided into orbitals.

In surface science, the study of reactivity sometimes has to be done by using only knowledge of its properties without any information about the interacting adsorbate-metal system. The density of states was found to be a good analysis tool for this. In this case reactivity means that the more reactivity a metal surface has, the larger is the binding energy of an adsorbate. [6]

2.4 Molecular dynamics

Making dynamical simulation, which can be used beyond frozen substrate approximation, not only checks the accuracy of the calculated PES, but also gives more information about the adsorption process [24]. Quantum molecular dynamics (QMD) was first developed by Car and Parrinello in 1985. Another method used in molecular dynamics simulations is Monte Carlo method, but unlike in MD (molecular dynamics), dynamical properties can not be measured by using it. In MD simulations atoms are allowed to move in compliance with laws that define forces. To be exact, the motion can be described by Newton's second equation

$$\vec{F} = m\vec{a}, \tag{1}$$

which means that for a constant mass (m), force (F) equals mass times acceleration (a). Another formulae used in MD simulations are Lagrangian and Hamiltonian. By definition, MD is a numerical integration of the equation of motion and dynamical behaviors can be measured by taking appropriate time averages over the simulation. [25]

In this study 300 K surface temperature controlled by Nosé thermostat [26, 27] is used. Nosé thermostat handles modifications of equations of motion with differential feedback control, but permits fluctuations in the momentum temperature. In the calculations kinetic energy of 25 meV was used for the molecule, timestep of 3 fs was used for the first simulation round and 1 fs after that.

3 Parameters and testing

Before starting actual calculations, the input parameters for the SIESTA and VASP programs should always be carefully tested. Parameter testing for SIESTA includes calculations for finding out cut-off energies and amounts of K-points, which have a pivotal role in the accuracy of calculations. Lattice constant and bonding distance for copper and oxygen are also calculated to find out the reliability of pseudopotentials. For VASP several calculations were also made to test the reliability of PAWs and the results of testing are introduced below. Proper supercells for different situations are also chosen.

3.1 Testing for SIESTA

3.1.1 Calculational supercells

When surfaces are studied, a proper three-dimensional approach has to be formed in order to introduce the actual surface with periodic structure. This can be done by using a so-called slab approach, the idea of which is shown in figure 6. In this method the material is replaced by a slab with two surfaces and a finite number of layers, which leads to a 2-dimensional lattice. To gain 3-dimensional periodicity for the calculations, a sufficiently large amount of vacuum is added between the slabs and thus a supercell is formed. The vacuum region must be large enough to separate the surfaces of the slab and to avoid interactions of opposing surfaces or adsorbates. The slab has to be also thick enough to model bulk states and surface relaxations.

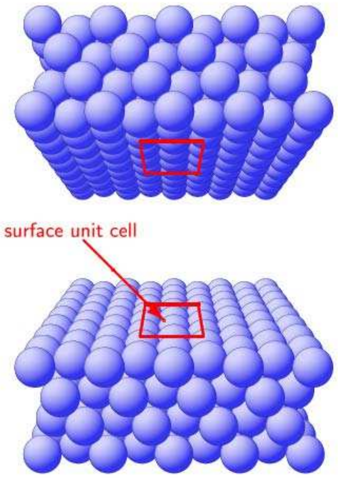

Figure 6: The idea of a supercell approach [6].

In this work copper is modeled by two different kind of supercells for calculations made with SIESTA. The size of the supercell is one of the fundamental problems in computational modelling of materials, because the size is strictly restricted by computational resources and despite that the supercell, as it was mentioned, should be large enough. First supercell, which is shown in figure 7 on the left, includes 3×3×6 atoms and the Miller index of the surface is (100). Figure 8 on the right shows the supercell for Cu(211) structure, which includes 36 atoms. The amount of vacuum was tested to be sufficient for the both cells in order to depicts infinity.

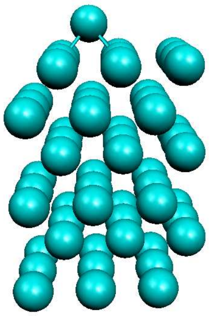

Figure 7: Supercell for Cu(100) structure with a copper adatom.

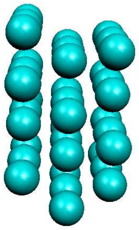

Figure 8: Supercell for Cu(211) structure.

When the supercell is formed, lattice constant is used for placing the atoms to their positions. Those positions are not, however, the most favorable ones in a system and usually in the case of metal surfaces the first atom layer relaxes downwards when the energetic minimum of the system is gained. Due to that the surface has to be relaxed before further calculations. As the adsorption process is modeled only for one side of the slab, the accuracy of the model can be improved by keeping some of the layers on the other side fixed at their bulk positions. [6]

When Cu(100) structure with copper adatom was let to relax, the adatom relaxed to 1.6 Å distance from the first layer and the first layer relaxed 0.07% upwards from it's original place on an average. For clean Cu(100) we got 0.95% relaxation of the first layer compared to the experimental result of 1.2% [28]. In the case of Cu(211) surface, the first layer of step and row marked with 3. in figure 9 relax upwards 0.02% and the row between them (2.) relaxes downwards 0.8%.

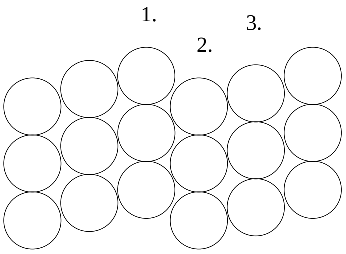

Figure 9: Structure of the Cu(211) surface.

3.1.2 Pseudopotentials and basis sets

The use of norm-conserving pseudopotentials significantly reduces the computational effort and simultaneously maintains an accurate description for most systems. In this case Troullier-Martins [9] type of pseudopotentials are used and they and the basis set were tested by A. Puisto [29]. Those tests show that pseudopotentials are suitable for further calculations, because calculations which were made with them gave 3.69 Å lattice constant for copper and 1.237 Å bond length for oxygen molecule, while experimental values for copper and oxygen are 3.61 Å and 1.207 Å, respectively. Basis set for the copper is also optimized and convergence tests for the shape and size of the basis orbitals of the oxygen molecule showed that adding d-like orbitals to the basis of the oxygen leads to a better convergence than using orbitals with s and p symmetry only. [29]

3.1.3 Mesh cut-off and k-points

Choosing the k-points for calculations affects also remarkably the accuracy of calculations due to the fact that k-points represent the sampling of the first Brillouin zone (1BZ) in the k-space, which is actually the primitive cell in k-space. This primitive cell is a so-called Wigner-Seitz cell, which is defined as the region of space around a lattice point that is closer to that lattice point than any other lattice point. K-points that we use in calculations are just a part of allowed k-points in the 1BZ and they should be chosen along the size and symmetry of the slab. The bigger the slab is, the less k-points are needed. Dimensions that are more broken in symmetry than others need also more k-points. So for a slab with vacuum in the z direction, there is no significant antisymmetry in this direction and it is enough to use only a one k-point. For the x and y directions in the surface plane, a finite k-point mesh has to be determined which accurately reflects the bulk band structure of the metal studied.

In this study Monkhorst-Pack [30] scheme for k-points sampling is used. For the slab with (100) surface A. Puisto [29] has calculated a suitable amount of k-points ($6\times6\times1$), which we use also in this study. Mesh cut-off, which is also chosen by Puisto, is 400 Ry.

Both of these parameters, amount of k-points and cut-off, should be large enough to ensure the accuracy of the results, but on the other hand they should not be too large, because it leads to waste of computational time. Large values can actually produce more incompetent results as can be seen in the table 1, in which total energies calculated with different amounts of k-points are shown. This is due to the shape of Brillouin zone and its irreducible part which determine the optimal set of k-points. These calculations were made by using the slab, which has a (211) surface structure. The table shows that differences between total energies are very small, but $8\times8\times1$ k-point grid was chosen, because it seems to be the most suitable for further calculations.

6×6×1	8×8×1	8×8×2	9×9×1
-56986.845	-56986.850	-56986.850	-56986.831

Table 1: Total energies for Cu(211) slab relaxation calculations with different amounts of k-points.

3.2 Testing for VASP

3.2.1 Supercells and k-points

Several calculations, the more precise description and results available elsewhere [31], were made in order to find out the suitable amount of layers for the supercells. Also amount of k-points was tested and chosen to be 6×6×1.

For the first actual calculations with VASP three different supercells with 6 atom layer were formed: the first one has eight copper atoms, the second has one silver and seven copper atoms and the last one has eight silver atoms in the first layer. In table 2 distances of relaxed layers of a structure containing only copper are shown. Percentages tell the magnitude and direction of relaxation and as can be seen from the values, the first and fifth layers relax most significantly, about 3 % downwards.

Layer	Distance	Relax [Å]	Relax [%]
1.	1.767	-0.053	-2.935
2.	1.829	0.009	0.467
3.	1.831	0.011	0.580
4.	1.828	0.008	0.424
5.	1.766	-0.054	-2.948
6.	Fixed	Fixed	Fixed

Table 2: Relaxation of a copper slab. Values have been calculated by subtract calculatory distance of layers (1.82 Å) from a distance got from relaxed layers. Negative values mean relaxation downwards and positive upwards. The bottommost layer is fixed.

In table 3 results from the relaxation calculations of silver doped copper are exhibited. The values obtained for copper surface with one atom substituted with silver atom are almost the same as values got from clear copper surface. The first and second lowest layers relax slightly downwards and the other layers relax a bit upwards. The relaxation of the first layer is smaller when using silver doped copper surface than if a clean copper surface is used. However, the relaxation in a slab with monolayer of silver differs from the results above. The first layer relaxes about 16% upwards to attain the 2.12 Å layer distance. This is caused mainly by the lattice constant of silver which is bigger than that of copper and the distance of two silver layers would thus be 2.08 Å .

7 Cu 1 Ag			8 Ag		
Distance	Relax [Å]	Relax [%]	Distance	Relax [Å]	Relax [%]
1.809	-0.011	-0.591	2.119	0.299	16.410
1.830	0.010	0.576	1.805	-0.015	-0.845
1.836	0.0156	0.856	1.821	0.001	0.070
1.833	0.013	0.695	1.814	-0.006	-0.346
1.771	-0.049	-2.704	1.752	-0.068	-0.346
Fixed	Fixed	Fixed	Fixed	Fixed	Fixed

Table 3: Relaxation in slabs. The bottommost layers are fixed.

For calculations made for examination of segregation phenomena three additional supercells were formed. In these cells there are only 5 atom layers and 4 atoms per layer in order to simplify the calculation processes. The structure of the cells is $(\sqrt{2} \times 2\sqrt{2})R45^{\circ}$ and in all of them one layer containing only copper atoms is replaced with silver atoms.

In tables 4 and 5 the relaxation values of the slabs are exhibited. As can be seen from the numbers, silver layers relax upwards 16-17%. Silver layers also induce the relaxation of the upper copper layer, which is about 14-16%. As mentioned earlier, this is partly caused by a bigger size of the silver atoms.

Surface	4 atoms		4 atoms		
	Relax [Å]	Relax [%]		Relax [Å]	Relax [%]
1 layer, Cu	0.269	14.757	1. layer, Ag	0.293	16.120
2. layer, Ag	0.310	17.052	2. layer, Cu	-0.019	-1.021
3. layer, Cu	-0.009	-0.470	3. layer, Cu	-0.006	-0.307
4. layer, Cu	-0.064	-3.490	4. layer, Cu	-0.074	-4.016
5. layer, Cu	Fixed	Fixed	5. layer, Cu	Fixed	Fixed

Table 4: Relaxation in copper slabs with silver in various layers.

As can be seen from the results below the first copper layer relaxes about 3% downwards in the situation of clear copper surface. This is consistent with the result calculated with a bigger slab containing eight copper layers. When the third copper layer is substituted with a silver layer, the first and fourth layers relax downwards about 5% and second and third layers upwards 16%.

Surface	4 atoms		4 atoms		
	Relax [Å]	Relax [%]		Relax [Å]	Relax [%]
1. layer, Cu	-0.082	-4.490	1. layer, Cu	-0.053	-2.916
2. layer, Cu	0.292	16.064	2. layer, Cu	0.023	1.258
3. layer, Ag	0.293	16.103	3. layer, Cu	0.028	1.539
4. layer, Cu	-0.094	-5.186	4. layer, Cu	-0.029	-1.616
5. layer, Cu	Fixed	Fixed	5. layer, Cu	Fixed	Fixed

Table 5: Relaxation in copper slabs with and without silver.

3.2.2 Lattice constants

The first part of the PAW testing was accomplished by three simple calculations. Lattice constants for bulk silver and copper and bonding distance for the oxygen molecule were computed. The experimental value for the lattice constant of copper is 3.61 Å and the calculated one was only slightly bigger, 3.64 Å. Also the lattice constant of silver was pretty accurate, because the calculated value was 4.15 Å while the experimental value is 4.09 Å. Finally the oxygen molecule was allowed to relax to its bonding distance and the result was also proper 1.235 Å when the experimental value is 1.207 Å . The result for oxygen was also more accurate than the value calculated with ultrasoft pseudopotentials if we compare them to the experimental value [22]. Below, plots for the lattice parameters of copper and silver are shown in figures 10 and 11.

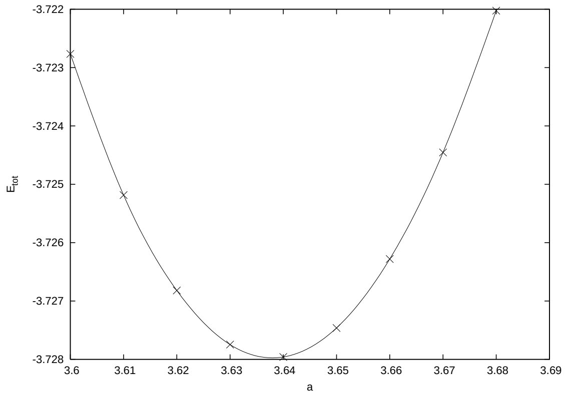

Figure 10: Calculated lattice constant of copper. The value can be seen from the point where the energy reaches its minimum, -3.73 eV.

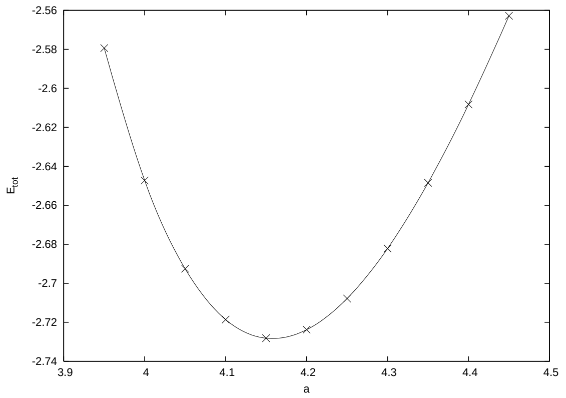

Figure 11: Calculated lattice constant of silver. In this case the minimum energy is -2.72 eV and the value of the lattice constant is 4.15 Å.

3.2.3 Cohesive energy

Cohesive energy describes how much energy is needed to get two atoms in a crystal infinitely far away from each other. The value was calculated with the following equation

$$E_{cohesive} = E_{atom,free} - E_{atom,bulk}, \tag{2}$$

where $E_{atom,free}$ means the energy of a free atom and $E_{atom,bulk}$ means the energy of an atom in bulk. Figure 12 below shows the calculated energy of a free atom related to the size of a supercell.

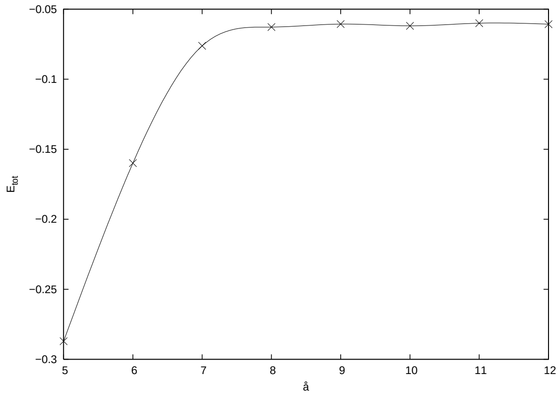

Figure 12: Energy of a single copper atom calculated with a supercell the size of which was increased gradually.

Experimental result for cohesive energy is 3.5 eV [32] and the one calculated for this study is quite accurate as its 3.79 eV. One can notice not only from this but also previous results that PAWs for oxygen, copper and silver are suitable for further calculations.

3.2.4 Bulk modulus

The bulk elastic properties of a material determine how much it will compress under a given amount of external pressure. The bulk modulus, B, is a material property that relates the change in volume with a change in pressure. Bulk modulus is the second derivative of the lattice constant calculations and it is defined by equation

$$B = \Omega \frac{d^2 E}{d\Omega^2}, \tag{3}$$

where Ω is the volume and E is the total energy. As a last test for a PAW of copper the result was also suitable 151.9 GPa while the experimental figure is 140 GPa.

3.2.5 Cut-off energy

The cut-off energy, as it has been mentioned earlier, is one of the most important parameters to be tested. It describes the amount of plane waves in the calculations and it should be large enough, because too small cut-off energy is a potential source of errors. From another direction the cut-off energy characterizes the energy of the last term in the cutted series which describes the wave functions. If it is too large the calculation time is yet again wasted. As can be seen in figure 13, PAW for oxygen converges slowly. Oxygen needs higher cut-off energy than copper and silver, so a 430 eV cut-off energy was used in all calculations made for this study with VASP.

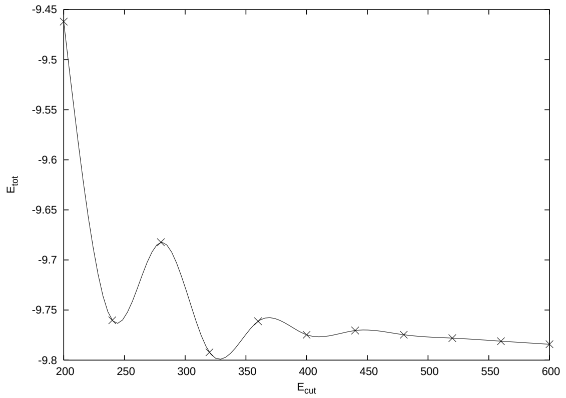

Figure 13: Total energy for an oxygen atom as a function of the cut-off energy.

4 O_2 adsorption on structurally modified Cu(100)

In this section previous studies and results from calculations made for researching oxygen adsorption on structurally modified copper surface are introduced. In this case vacancies and adatoms are used in order to modify the copper (100) surface and calculations for vacancies are made by A. Puisto [29]. In the result section some DOS figures, several elbow plots of PES and results from MD simulations are shown.

4.1 Previous studies

The adsorption dynamics of O_2 on clean Cu(100) were studied by Alatalo et al. [2] and their study stated that after the oxygen induced reconstruction the dissociation of the oxygen molecule is prevented by the on-surface oxygen. Due to that, oxygen ends up to the molecularly adsorped state on the hollow site, which has the largest adsorption energy according to PES calculations and also MD simulations starting from several configurations lead to the same result with small kinetic energies. If the molecule has enough kinetic energy, it will, however, dissociate directly along the calculated PES trajectories.

Junell et al. [33] added surface modifications to the same surface and studied their effect on the adsorption dynamics with molecular beam surface scattering (MBSS) technique. They found that surface defect sites are responsible for the O_2 adsorption on clean and structurally modified Cu(100) at low translational energy. On the other hand, surface defects do not play a markable role in the adsorption at high translation energy.

4.2 Results

In this section the results of the PES, DOS and MD calculations are shown. The contour lines are drawn at intervals of 0.1 eV in all the PES plots shown in this study.

Figure 14 shows the PES for O_2 approaching the top site of a copper adatom. This situation is also shown on the left hand side of figure 15.

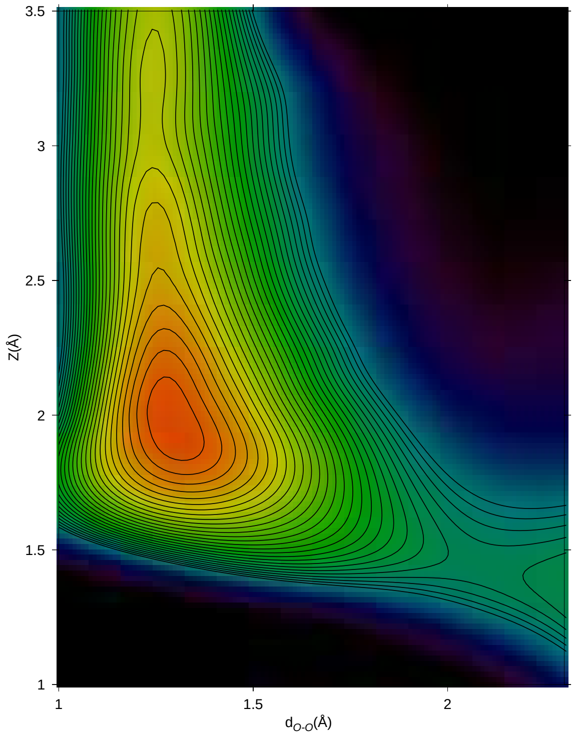

Figure 14: PES for oxygen molecule approaching the top site of a copper adatom.

As can be seen from the PES the barrier is 2.3 eV in the dissociative pathway, which indicates that dissociation does not occur. The plot is otherwise similar to the PES on clean Cu(100) [2], but the barrier is much larger in this case.

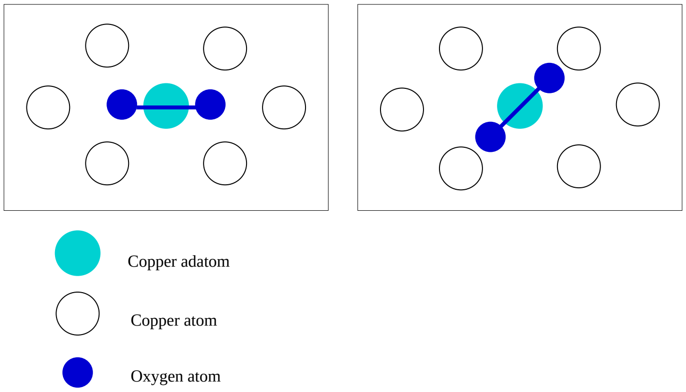

Figure 15: Positions of the oxygen molecule in the case of an adatom. The light blue atom represents the adatom on the surface.

In figure 16 the PES from situation shown on the right hand side of the figure above is shown. The deflection of the oxygen molecule affects the PES only slightly: the PES seems to be almost similar to the previous PES, only the barrier is 0.2 eV smaller.

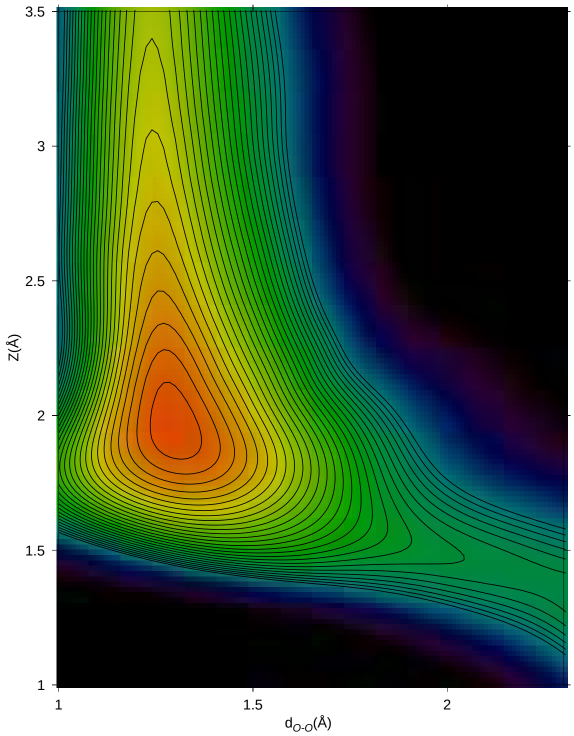

Figure 16: PES for the oxygen molecule approaching top site of the adatom.

In addition to the PES calculations some local density of states plots were calculated. In the first figure 18 d-DOS for the copper adatom and p-DOS for the oxygen molecule approaching the adatom are shown. In DOS figures the upper mark in the x-axis represents the Fermi level and the lower one represents the value -20 eV. Also, the points where the DOS figures are plotted are shown in figure 17.

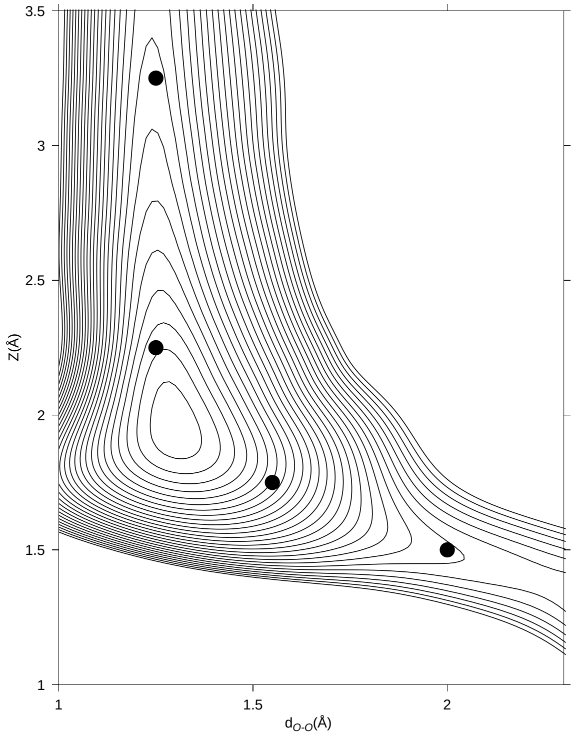

Figure 17: Points where the DOS figures are drawn.

As the oxygen molecule approaches the adatom, some bonding between the adsorbate and subtrate can be seen from the DOS below.

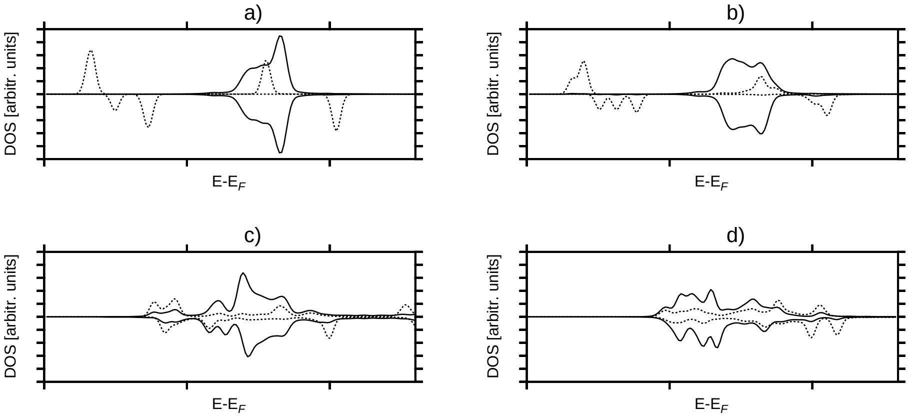

Figure 18: DOS figure where d-DOS for the adatom and p-DOS for oxygen are plotted.

in figure 19 the d-DOS of the nearest copper atom from the adatom and p-DOS for oxygen are plotted. As can be seen in the figure, these atoms do not affect each other notably as they are so far away from each other, which leads to a larger dissociation barrier for the oxygen molecule than in the case of clean Cu(100).

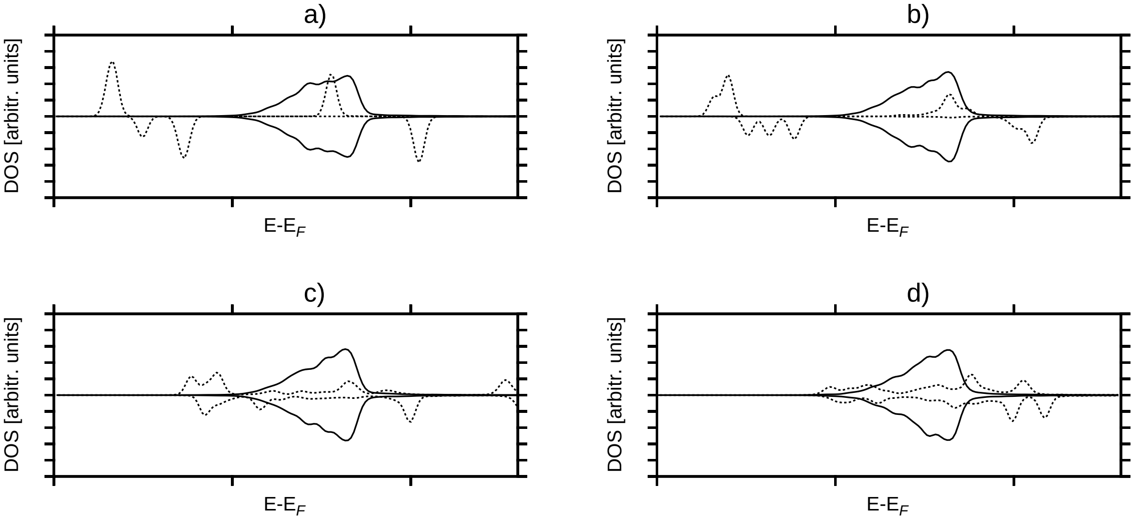

Figure 19: DOS figure where d-DOS for the nearest copper atom and p-DOS for oxygen are plotted.

Next, results from the calculations regarding the adsorption of an oxygen molecule on a surface with vacancies are shown. The positions of the oxygen molecule can be seen in figure 20 where the left figure shows the situation from the PES 21 with a vacancy and the one on the right represents the situation in the PES 22 with divacancy.

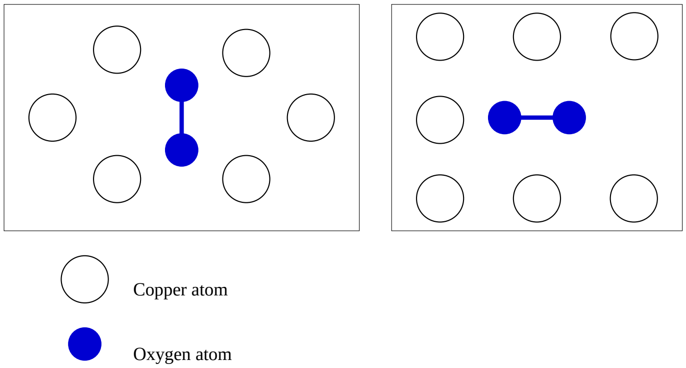

Figure 20: Positions of the oxygen molecule in the case of vacancies.

The PES in figure 21 indicates dissociation of the oxygen molecule as there is no barrier in the pathway. This was also shown in the molecular dynamics simulations. Also PES 22 shows the possibility of dissociation although there is a small barrier.

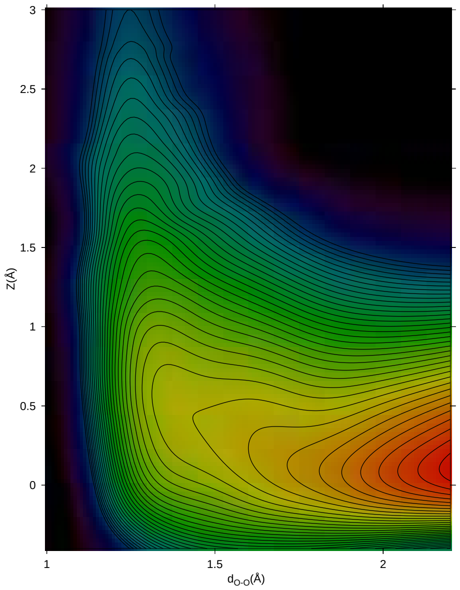

Figure 21: PES for the oxygen molecule approaching vacancy from straight above.

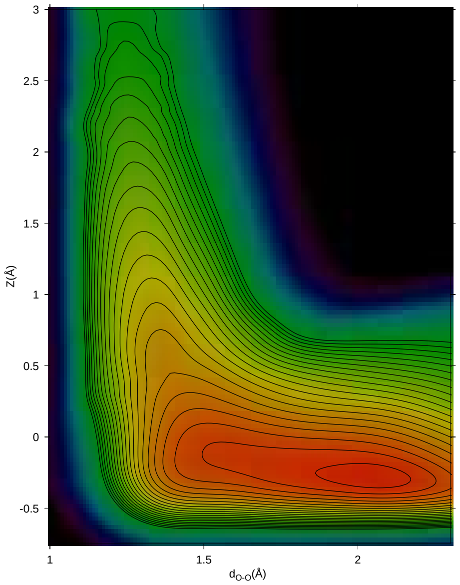

Figure 22: PES for the oxygen molecule approaching divacancy from straight above.

The next PES is from the situation where oxygen molecule approaches the top site of an atom next to a vacancy. As can be seen from the PES below figure 23 vacancies are more dissociative than the copper atom next to them.

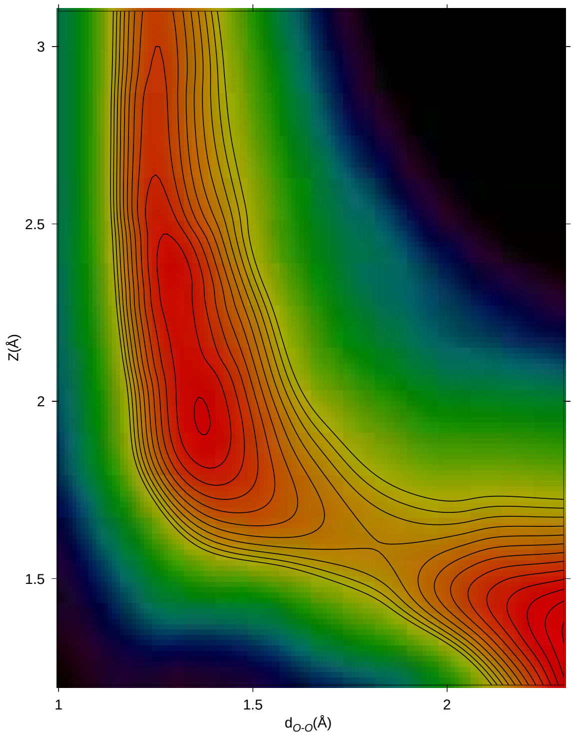

Figure 23: PES for the oxygen molecule approaching top site of a copper atom next to the vacancy.

In order to study how far vacancies affect the adsorption process, some molecular dynamics simulations, where the oxygen molecule approaches an atom next to a vacancy were performed. When the oxygen has the bridge-hollow-bridge (b-h-b) starting position, the molecule adsorbs into the vacancy but the vacancy moves away from the molecule and a copper atom takes the free place as can be seen from figure 24.

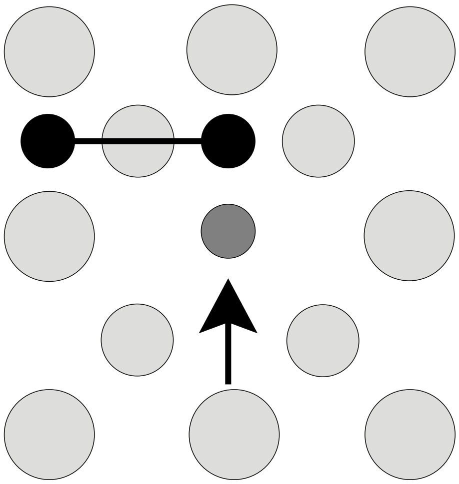

Figure 24: Approaching oxygen molecule causes the vacancy diffusion away from the molecule.

4.3 Conclusions

As the results showed, adatoms have an inhibitive impact on the dissociation of the molecule and, on the other hand, vacancies act as dissociative centres. In the case of adatoms the barrier is higher than the barrier which exist when oxygen adsorbes on a clean surface. This is explained by the nearest copper atoms, which are further away from the oxygen when the molecule moves straight towards an adatom on a surface. Vacancies increase the dissociation possibility and an interesting phenomenon was also found when a molecular dynamics run with the starting orientation of h-b-h showed that the oxygen molecule causes diffusion of vacancies.

5 Adsorption of atomic oxygen on Ag/Cu(100)

In this section several calculations were made by using both clean and silver precovered copper surface. The calculations made with the clean surface are made mainly for comparison and they offer a possibility to find out if the results obtained using ultrasoft pseudopotentials [22] and PAW calculations differ from each other. Although total energies obtained from different programs are not comparable, the trend of the results should be the same. The main goal, however, is still to explain how silver affects the oxygen adsorption in a copper surface.

The alternative adsorption sites for Cu(100) surface are called hollow, bridge and top which discribes the position of the adsorped atom on a surface. Adsorption energies were calculated with all of these sites to find out which one of them is the most favourable for oxygen adsorption and the equation used for computing is

$$E_{ads} = \frac{\left(E_{tot} - E_{clean} - \frac{N_o}{2} \cdot E_{O_2}\right)}{N_o}, \tag{4}$$

where N_o is the amount of oxygen atoms and E_{O_2} is the energy of an oxygen molecule.

In table 6, the calculated adsorption and total energies for all the systems are shown. In the system with 7 copper and one silver atoms in the first layer the adsorped oxygen atom is near the silver atom. It can be seen from the energies that the hollow site is the most favourable adsorption site in all situations. In the case of the clean copper surface the adsorption energies are almost similar to the values got from the calculations made with ultrasoft pseudopotentials [22]. Oxygen atoms adsorb more likely to copper surface than to surfaces containing both copper and silver. Results show also that the more silver there is on a surface, the smaller adsorption energy the oxygen atom has. This could indicate the silver's inhibiting impact on copper oxidation.

Surface atoms	Site of O	$E_{tot}[eV]$	$E_{ads}[eV]$
7 Cu,1 Ag	Top	-172.301	+1.010
7 Cu,1 Ag	Bridge	-174.083	-0.773
7 Cu,1 Ag	Hollow	-175.159	-1.848
7 Cu,1 Ag	2. Layer	-173.265	+0.046
8 Ag	Top	-164.539	+0.961
8 Ag	Bridge	-165.378	+0.122
8 Ag	Hollow	-166.070	-0.57
8 Cu	Top	-174.245	-0.102
8 Cu	Bridge	-175.482	-1.339
8 Cu	Hollow	-176.229	-2.086

Table 6: Total and adsorption energies of all the surfaces studied.

The following DOS-figures were drawn to find out the effects of adsorbing oxygen on silver and copper. Influences of silver were also examined. For oxygen atom only p-DOS is drawn and for copper and silver atoms only d-DOS is drawn. DOS-figures 25 and 26, first of them with oxygen and second one without, show that oxygen affects the orbital stucture of copper, but the effect on silver is not so clear.

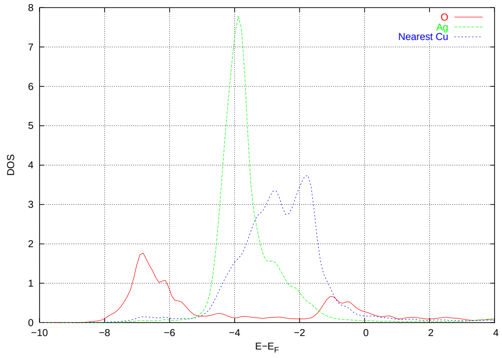

Figure 25: DOS for the situation where seven copper atoms and one silver atom are in the first layer and an oxygen atom is in the second layer and near the silver atom.

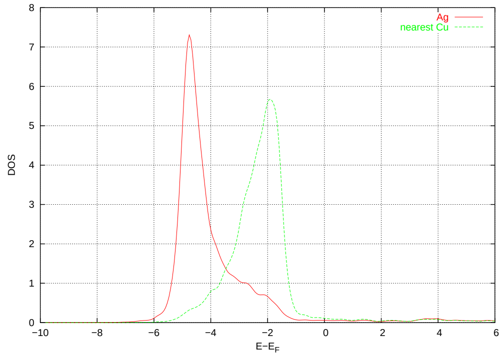

Figure 26: DOS for the situation where seven copper atoms and one silver atom are in the first layer.

If the situation of DOS figure 25 is examined more closely, it can be noticed from the electron density figure 27 that silver rises away from the surface in the presence of oxygen. Silver also pushes oxygen towards copper.

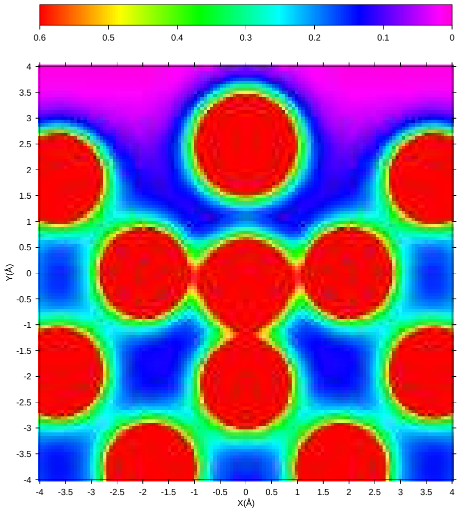

Figure 27: Electron density figure for the same situation as in figure 25. The biggest atom is a silver atom, the one straight below is an oxygen atom and other ones are copper atoms.

An electron density figure was also drawn for the case without oxygen 26. It can be seen from figure 28 that the bonds between copper atoms are stronger than the bonds between silver and copper atoms.

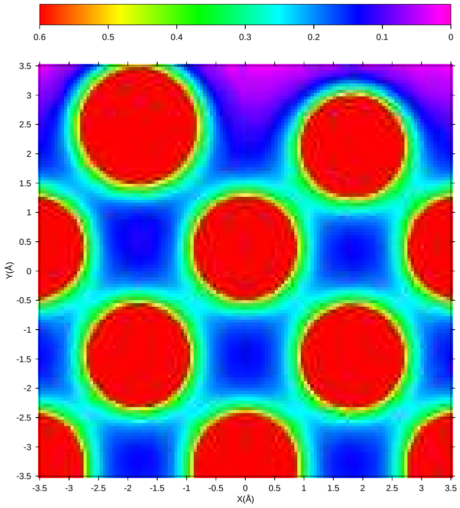

Figure 28: Electron density figure for the same situation as in the figure 26. The biggest atom is a silver atom and other ones are copper atoms.

5.1 Segregation

In this section oxygen induced segregation of the Ag/Cu(100) surface is investigated. At first, some results of previous studies are exhibited.

Experimental studies of Ag/Cu(100) have recently revealed an interesting segregation phenomenon [34, 35, 36]. If there is oxygen on this kind of surface copper segregates to the surface and forms an energetically favourable alloy of copper and oxygen. After that the topmost layers are copper and oxidation continues in the same way as on the unalloyed copper surfaces. The segregation phenomenon has also been studied theoretically with palladium based alloys by Løvvik [37]. They have found that both geometric and electronic effects are needed to explain the segregation. The smaller size of the substituted atom and the larger experimental surface energy of the metals, the more extensive the surface segregation is. Another interesting theoretical investigation comprises Monte Carlo simulations of adsorption induced segregation [38]. The most important result was that the adsorption of O and CO can significantly change the surface composition of bimetallic alloys. Adsorbent induced segregation has also been found in a study of methanol synthesis on the Ni/Cu(100) surface [39].

In the following segregation calculations, oxygen atoms were placed on the hollow sites, since it is the most favourable site for the oxygen adsorption on this kind of surfaces. This is shown not only in this study but the result agrees also with the previous studies [40, 41]. As can be seen from the total energies in table 7, the first layer is the most favourable position for silver atoms. The presence of oxygen makes the situation completely different: total energies are more negative when silver goes towards the bulk. If there is a 0.25 ML oxygen concentration on the surface, the difference between total energies is 3.25 eV. When the oxygen concentration rises, the difference between total energies also increases. Thus silver diffuses towards the bulk when oxygen concentration goes up. When the coverage of oxygen is increased, the probability of adsorption decreases. This phenomenon has also been studied experimentally [34] and theoretically [42] by using a reconstructed surface and the results obtained from those studies agree with the results exhibited in this work.

n	Oxygen coverage (ML)	$E_{tot}[eV]$	$E_{ads}/atom[eV]$
-	0	-69.722	-
-	0.25	-76.637	-2.031
-	0.5	-82.798	-1.653
-	1	-92.255	-0.748
1.	0	-65.383	-
1.	0.25	-67.731	+2.537
1.	0.5	-70.926	+2.114
1.	1	-80.489	+1.109
2.	0	-63.803	-
2.	0.25	-70.980	-2.292
2.	0.5	-77.376	-1.901
2.	1	-87.391	-1.012
3.	0	-63.995	-
3.	0.25	-70.955	-2.075
3.	0.5	-77.103	-1.668
3.	0.75	-82.956	-1.435
3.	1	-86.519	-0.746

Table 7: Calculated total energies of different structures and adsorption energies for oxygen. The column titled n indicates which copper layer is replaced with a silver layer. The value for the energy of the oxygen molecule is -9.770 eV and it is used in the adsorption energy calculations.

In figure 29 DOS-diagrams for copper, silver and oxygen are on view. It can be seen in the DOS-plots that in the case of copper there exist more states near the Fermi level, so there is bonding between the nearest copper atom and the oxygen atom. The states of silver reside lower and therefore weaker bonding between silver and oxygen appears.

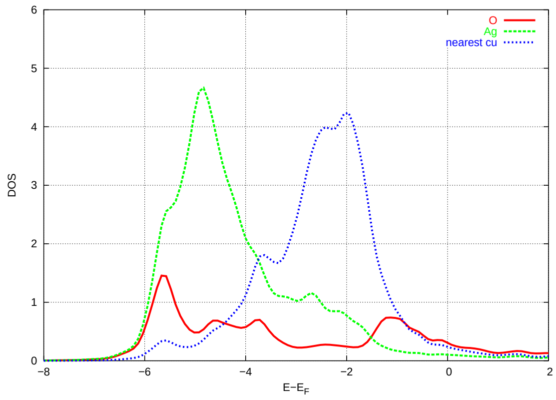

Figure 29: p-DOS for oxygen and d-DOS for copper and silver. The surface contains seven copper and one silver atoms with oxygen atom in the hollow site.

The situation from which figure 30 is plotted is otherwise the same as in figure 29, but instead of 1 silver atom there is a whole layer containing only silver atoms. Although some bonding between copper and oxygen can be seen, one can not clearly find antibonding between silver and oxygen. The states of silver reside upper in this case compared to the case with surface including only 1 silver atom.

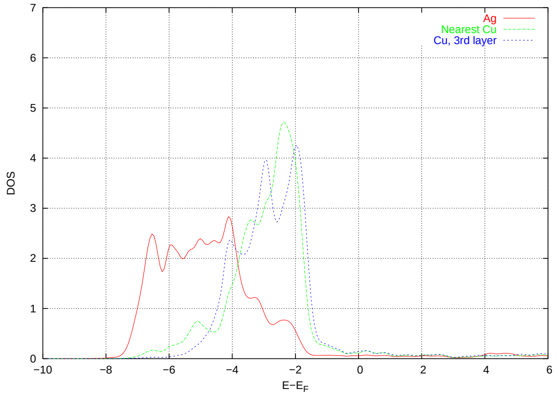

Figure 30: First copper layer is replaced with a silver layer.

Some electron density simulations were also run. It can be seen in figures 31 and 32 that oxygen forms a slightly stronger bond with copper than with silver.

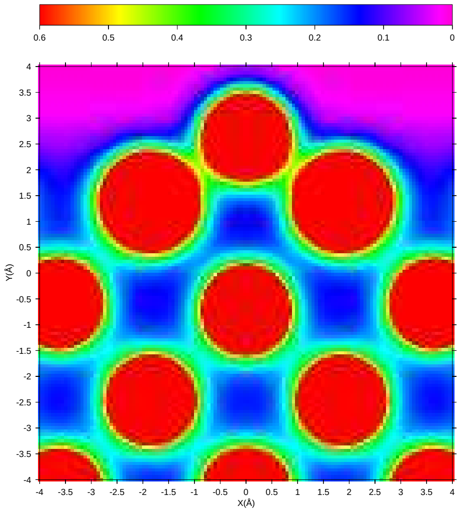

Figure 31: Electron density. The first copper layer is replaced with a silver layer and the uppermost atom is oxygen.

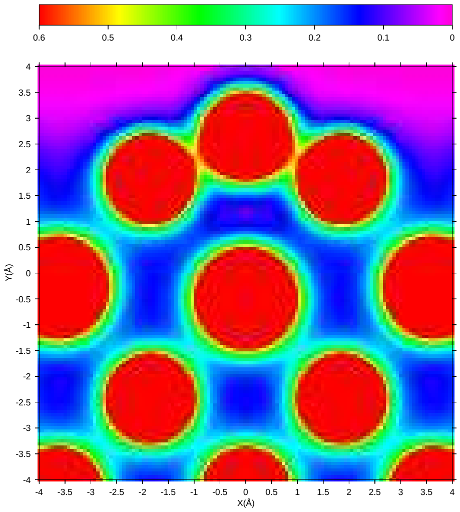

Figure 32: Electron density plot. The second copper layer is replaced with a silver layer and the uppermost atom is oxygen.

In figures 33 and 34 antibonding between silver and oxygen can be clearly seen.

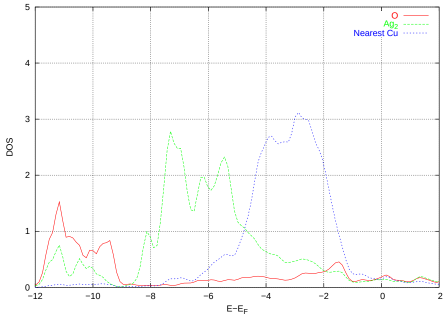

Figure 33: The first copper layer is replaced with a silver layer and there is an oxygen atom in the hollow site of silver atoms.

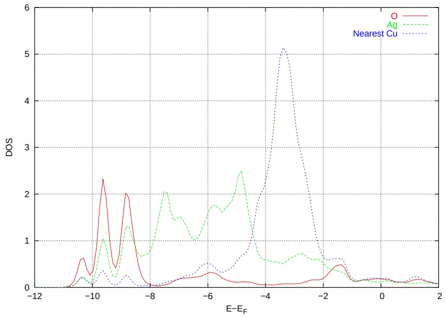

Figure 34: The second copper layer is replaced with a silver layer and there is an oxygen atom in the hollow site of copper atoms.

As it is impossible to estimate the most realistic lattice constant for a system with both copper and silver, the lattice constant of copper was used in previous calculations. Some test calculations were also made with bigger lattice constant and the trend of the results remained the same. We also changed the consentration of the layers, which again showed the trend of segregation. In addition to previous, calculations with 9 atoms in a layer were made and different k-point amounts tested. More information about the calculations and the results can be found in the references [31] and [42], the latter one includes also results obtained from calculations made with reconstructed copper surface.

5.2 Conclusions

All in all, several calculations were made to find out how silver affects oxygen adsorption on a copper surface. The most important result is that doping copper with silver does not inhibite oxidation. This is explained by the segregation phenomenon which occur during the oxidation process on a silver doped copper surface, which is also evidenced by the experimental studies.

In this chapter adsorption energies were calculated with different surfaces and the hollow site was found to be the most suitable site for the adsorption of atomic oxygen. Results also showed that oxygen adsorps more likely to pure copper surface than a copper surface doped with silver.

6 O_2 adsorption on Cu(211) surface

In this section results from calculations made for studying O_2 adsorption on the Cu(211) surface are introduced. The fact that steps make metal surfaces more reactive, stated for instance in the study made by Xu and Mavrikakis [43], makes steps worth further studying. This high reactivity can be explained by the amount of broken bonds which is much larger on stepped surfaces than low index surfaces.

In this case Cu(211) surface was chosen for the step surface calculations due to its (100)×(111) structure, which has been found to have high stability in a study made by Kollár et. al [1]. The (211) surface is also, as mentioner earlier, a simple and widely studied surface which is another advantage of using that surface. At first, short description of previous studies and some of the alternative research methods are presented.

6.1 Previous studies

Adsorption of different gases and other materials on Cu(211) surface has been recently studied by many authors. Especially the adsorption of carbon monoxide on Cu(211) has been under broad interest and it has been studied with both theoretical [44]-[46] and experimental [47] methods. In the study of Rouzo et al. [44], analysis of potentials and results of classical dynamics simulations were used for studying the migration and stability of CO on stepped surface and they found for instance that the migration of CO is favored along rows on Cu(211) surface. Gajdoš et al combined results obtained with Vienna *ab initio* simulation package (VASP) and scanning tunneling microscope (STM) and they found that CO molecules adsorb upright on the on-top sites at step edge atoms at low coverages up to 0.5 ML which was also stated by Marinica et al [45].

Another example of methods for adsorption studies is the spot profile analysis low energy electron diffraction (SPALEED) method, which is a surface-sensitive method that makes use of the diffraction of low-energy (typically 10-100 eV) electrons at a surface. The analysis of diffraction spot profiles affords for example information about terrace sizes and the number of atomic layers exposed to the surface. This method has been used for example by Braun et al. [48] who studied cesium adsorption on the Cu(211) surface. [49]

The most relevant papers for this work are studies of adsorption of O_2 on (211) step surface of copper as well as other materials. In this work we compare results obtained for Pd(211) surface [3, 50] to results obtained for Cu(211) in consequence of characteristics of palladium: it's a chemically reactive material and valence electron structures of palladium and copper are almost alike. Calculations with palladium are also made with the same methods as calculations in the present study, so the results of these studies are comparable.

The adsorption of O_2 on Cu(211) has been studied by Xu and Mavrikakis [43], who used density functional theory (DFT) based Dacapo method for their total energy calculations made for their study. Dacapo uses a plane wave basis for the valence electronic states and describes the core-electron interactions with Vanderbilt ultrasoft pseudopotentials. The program may perform molecular dynamics or structural relaxation simultaneous with solving the Schrödinger equations within density functional theory [51]. Xu et al. found for instance that all stable O_2 precursor states identified around a Cu(211) step adsorb much more strongly than those on Cu(111), which is consistent with the study made by Nørskov et al. [52] which showed that the adsorption of oxygen is increased at steps.

6.2 Results

In this section results from the calculations made for researching oxygen adsorption on the Cu(211) surface are introduced. These calculations offer us a possibility to compare copper and palladium surfaces as the same calculations are performed with both of them. The first six PES figures calculated with copper are shown in figure 35 and they are compared with the results obtained from calculations made with palladium surface, which are shown in figure 36.

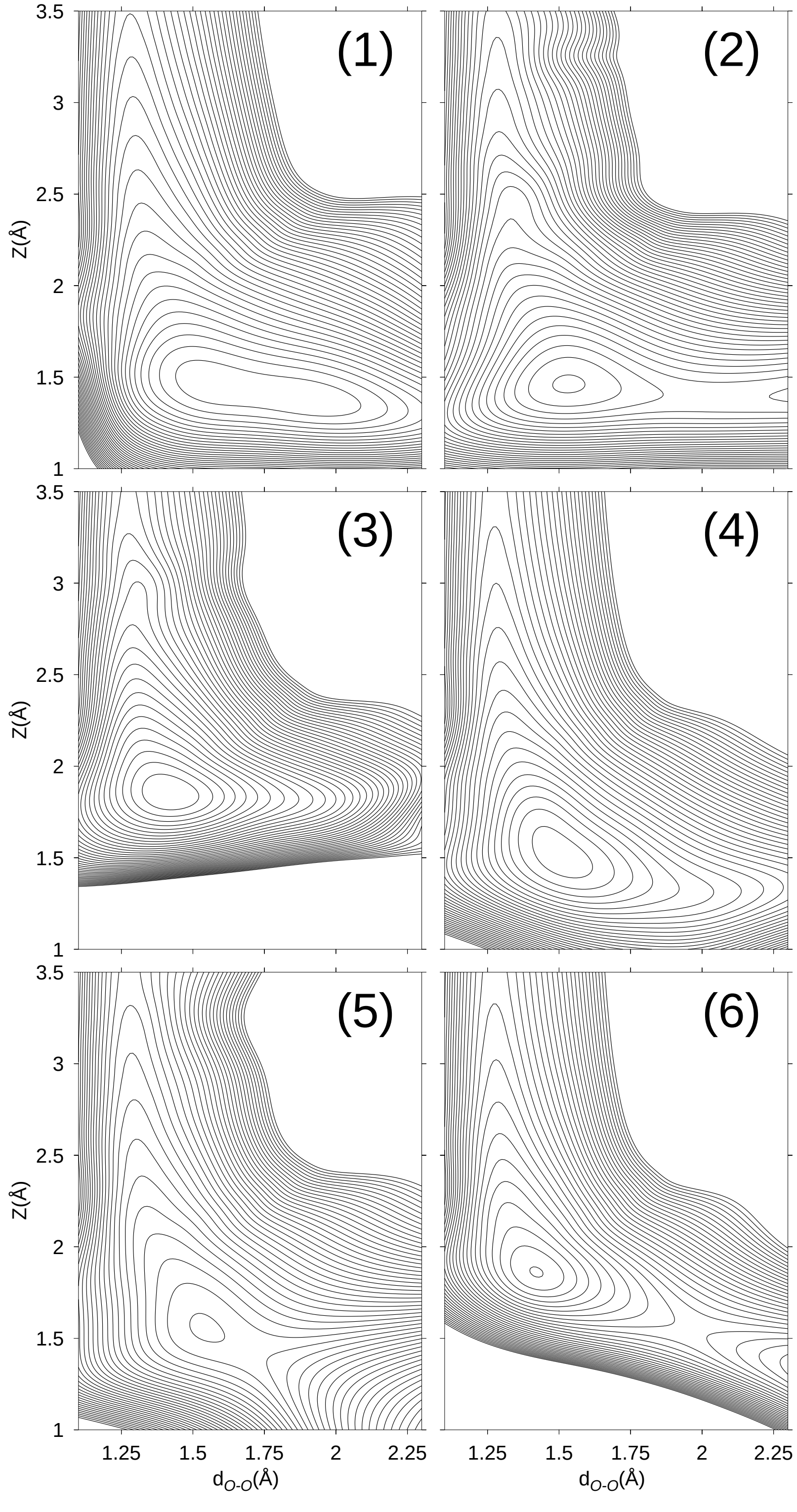

Figure 35: PES figures made for studying oxygen adsorption on Cu(211) surface.

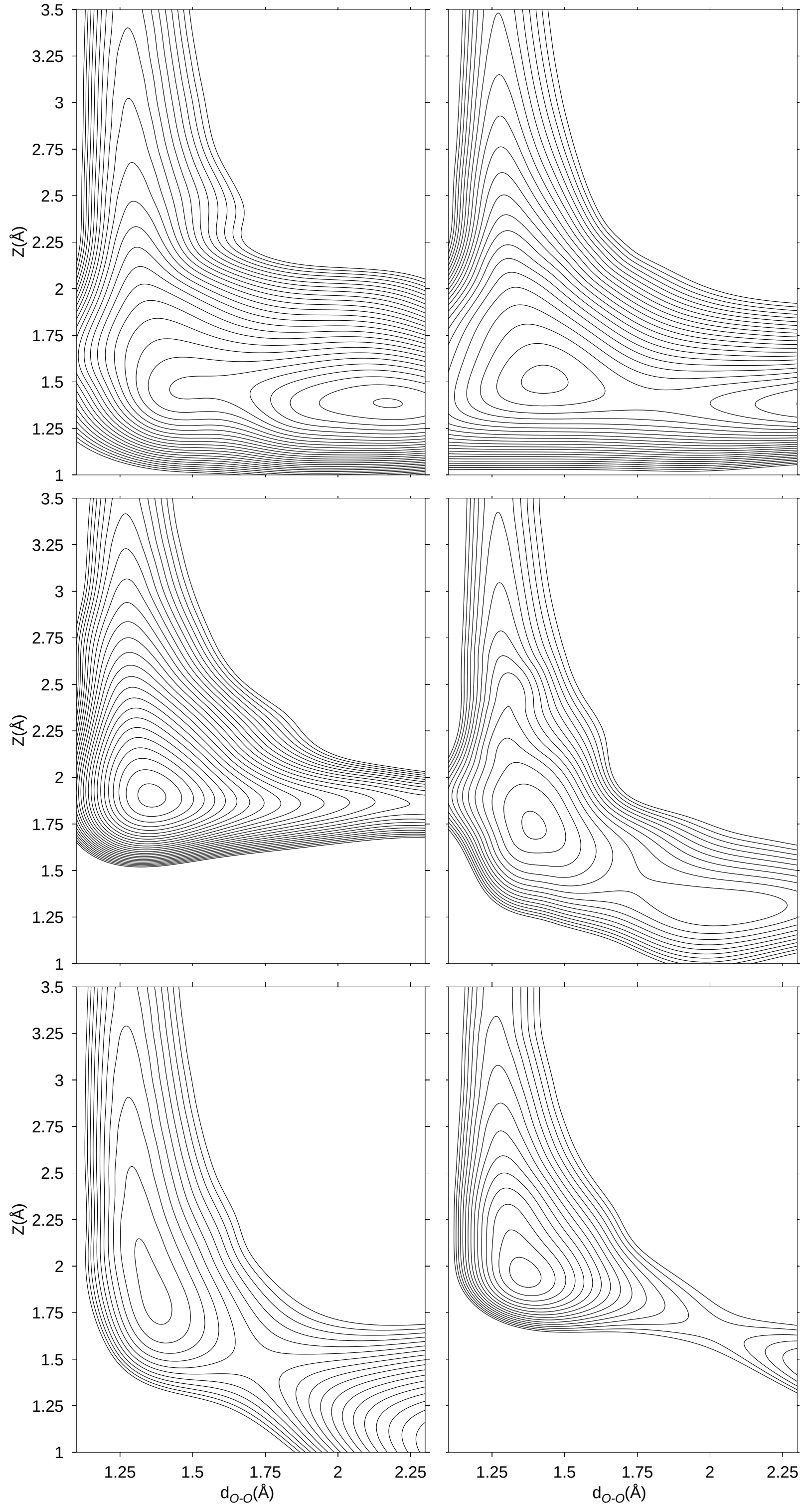

Figure 36: PES figures made for studying oxygen adsorption on Pd(211) surface [3].

Next, results shown above are analyzed and copper and palladium PES figures are compared with each others as matched pairs.

In figure 37 the situation for the first PES plots shown in figures 35 and 36 is shown. In this case the oxygen molecule approaches (100) microfacet's hollow site, which is the most dissociative site in the case of palladium surface, which can be seen from the PES 1 and 2 in the figure 36.

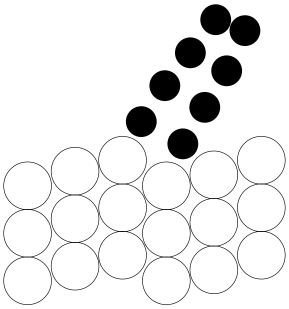

Figure 37: The oxygen molecule approaches the hollow site of the (100) microfacet in an orthogonal position.

As can be seen from the PES 1 in figure 35 the kinetic energy gain for the oxygen molecule is remarkably high at the entrance channel and there is only a small barrier at the dissociative pathway. In figure 38 almost the same trajectory as in the previous PES is shown, but in this case the oxygen molecule is deflected.

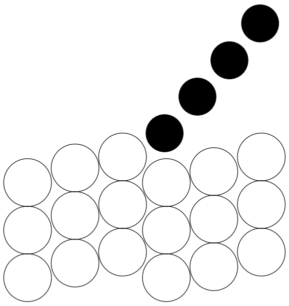

Figure 38: Oxygen molecule approaches straight (100)-microfacets hollow site.

The energy downhill is even bigger in this case than in the previous one, which can be seen from the second PES in figure 35. The late barrier is small, which also indicates dissociation. The third PES is from the bridge site on the step edge (top-bridge-top), which was found to be the most favorable site for molecular adsorption on the Pd(211) surface, which can be seen from the PES 3 in figure 36. The site is also an attractive site for the molecular adsorption in the case of copper as there is a large energy gain in the entrance channel as well as a big barrier in the dissociative channel.

The fourth PES in figure 35 is from the situation where the oxygen molecule approaches the bridge site on the step. The site is attractive, but as the barrier is large, the molecule is steered towards more favorable sites. In figure 39 an oxygen molecule approaching (100)-microfacet's bridge site can be seen.

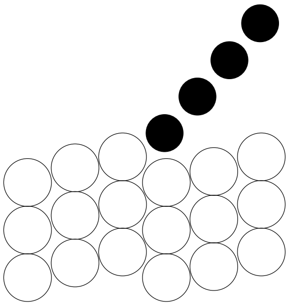

Figure 39: O_2 approaching the bridge site on the (100) microfacet.

The microfacet's bridge site was found to have only a small barrier in the case of palladium (PES 5 in figure 36), but since the PES showed a minimum at the hight of 2.5 Å the molecule is facing a steering effect towards the more favorable sites. When copper surface is examined the figure shows that the site is highly dissociative but not as dissociative as the hollow site on the same microfacet.

The last PES plots in figures 36 and 35 are from the step edge top site, where the molecule approaches the step along the normal vector of the (111) terrace. As can be seen from the figures, the minimums are so high, that the molecules are, as in the previous case, steered towards more favorable sites.

Figure 40 shows the situation for the PES (figure 41), where the oxygen molecule approaches the top site of the step with the orthogonal position towards (100)-microfacet.

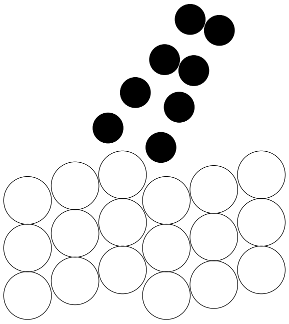

Figure 40: O_2 approaching the top site on the step with orthogonal position.

As can be seen from the figure below, the PES is almost similar to the previous case and deflecting the molecule doesn't change the result remarkably.

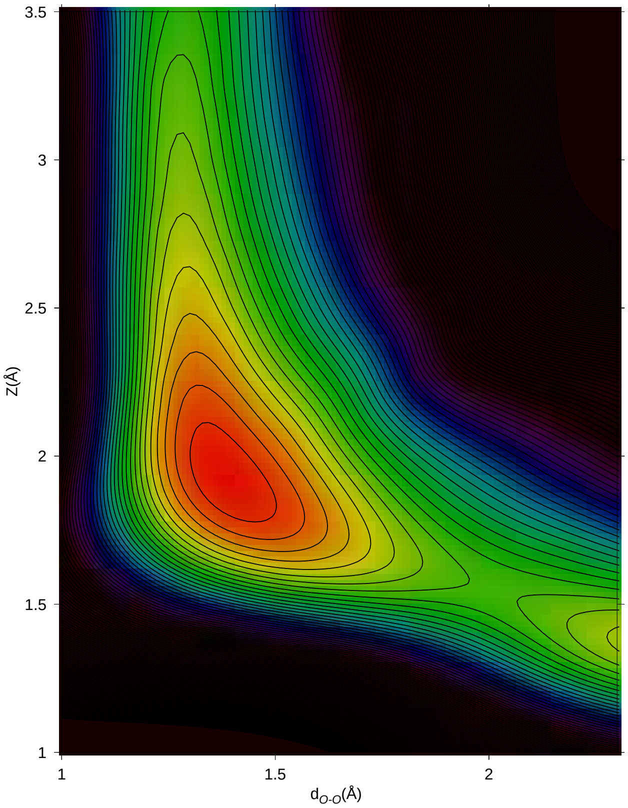

Figure 41: PES for the oxygen molecule approaching the top site on the step with orthogonal position.

As it was mentioned before, (100) surface is the most reactive low-index structure in the case of copper, so it can be assumed that (100) microfacet is more reactive than (111) microfacet. However, for comparison some PES calculations for the oxygen molecule on (111) terrace were calculated. The first one 42 represents the situtation, where the molecule approaches the top site of the terrace along the normal vector. As can be seen, PES shown in the figure below is almost similar to previous top site PES figures (40 and number six in figures 35 and 36).

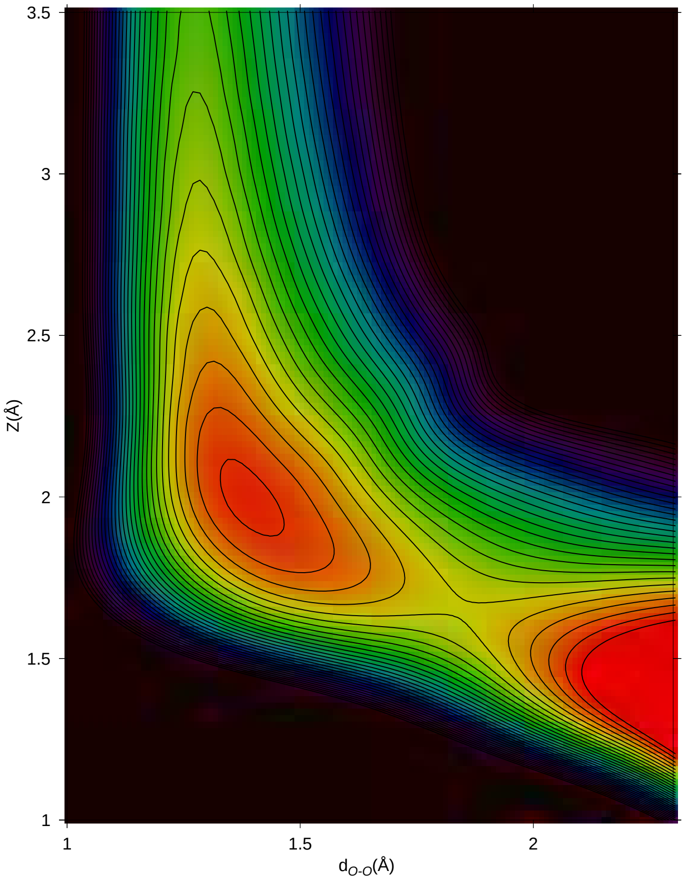

Figure 42: PES for the oxygen molecule approaching the top site on (111) microfacet.

Figure 43 shows the situation where the oxygen molecule approaches the FCC (Face Centered Cubic) hollow site, which was found to be the most favorable adsorption site for atomic oxygen on Cu(111) surface [53].

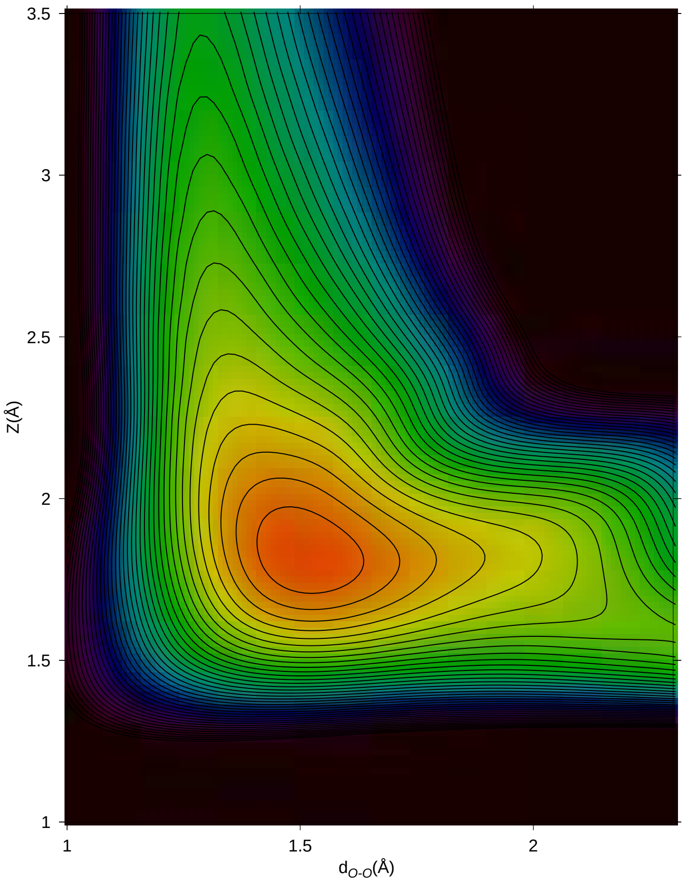

Figure 43: PES for the oxygen molecule approaching the FCC hollow site on (111) microfacet.

The shape of the figure is a bit similar than in the figure 1 in 35, which represents the situation from (100) microfacet's hollow site, but the minimum is lower in the latter case, and there is also a barrier in the dissociative pathway in this case. It can be assumed that the molecule is steered towards more favorable sites, but in order to get more specific information, some molecular dynamics simulations should be run.

6.3 Conclusions

As a conclusion of the previous section it can be stated that (211) step surfaces of copper and palladium are very reactive compared to their smooth surfaces. Pd(211) surface is more dissociative than Cu(211) while it has smaller dissociation barrier. The most favorable sites for dissociation are (100) microfacets' hollow sites and the bridge site on the step edge is the most attractive site for molecular adsorption. (111) terrace sites were also found to be less attractive than sites on (100) microfacet. As the steering phenomenon affects adsorption processes, further studies should include some molecular dynamics runs in order to find out the actual adsorption mechanism, as mentioned in the previous chapter.

7 Conclusions

In this study effects of steps as well as chemical and structural modifications on oxidation process on a copper surface were studied by performing different kinds of calculations. The calculations showed that structural modifications affect the adsorption process quite remarkably, but in this case the effects of chemical modifications are not so significant, as doping copper with silver doesn't prevent oxidation due to segregation phenomenon, which is also evidenced by experimental studies. The calculations performed for studying segregation were made with quite simple model, which offers a possibility to test if the same phenomenon exist when other materials are used. On the other hand, the model has its limitations as it is almost impossible to estimate e.g. the most realistic lattice constant for the whole system, so if the results obtained with this model show the trend of segregation, further calculations should be done in order to get some knowledge of the segregation process in more detail.

When the oxygen molecule approaches an adatom on a surface, the nearest copper atoms are further away from it than in the case of surface without adatoms, which leads to a smaller dissociation probability. The situation is, however, whole different when a surface contains also vacancies: molecules tend to dissociate above them.

When concerning an oxygen atom on Cu(100), the hollow site was found to be the most favorable adsorption site and for the oxygen molecule on Cu(211), the bridge site on the step edge and (100) hollow sites are the most attractive ones, which is also valid for Pd(211). As mentioned earlier, also some molecular dynamics simulations should be done to get more accurate information, but PES results can reveal the most interesting cases as MD simulations are time-consuming and thus all of the cases can not be simulated. Also oxidation on other (211) surfaces should be studied in order to get some general information about influence of steps on the process.

REFERENCES

[1] J. Kóllar, L. Vitos, B. Johansson, H.L. Skriver, Phys. Stat. Sol. b 217, 405, (2000).

[2] M. Alatalo, A. Puisto, H. Pitkänen, A.S. Foster, K. Laasonen, Surf. Sci. 600, 1574, (2006).

[3] M. Lahti, N. Nivalainen, A. Puisto, M. Alatalo, in press, Surf. Sci.

[4] P. Ordejón, E. Artacho and J. M. Soler, Phys. Rev. B (Rapid Comm.) 53, 10441, (1996).

[5] J. M. Soler, E. Artacho, J. D. Gale, A. García, J. Junquera, P. Ordejòn and D. Sànchez-Portal, J. Phys. Condens. Matter 14, 2745, (2002).

[6] M. Lischka, Adsorption of simple molecules on structured surfaces, PhD thesis, Technische Universität München, (2003).

[7] J. E. Lennard-Jones, Trans. of the Faraday Soc. 25, 668, (1929).

[8] G. B. Bachelet, D. R. Hamann, and M. Schlüter, Phys. Rev. B 26, 4199, (1982).

[9] N. Troullier, J.L. Martins, Phys. Rev. B 43, 1993, (1991).

[10] P. Ordejón, E. Artacho, J. M. Soler, J. D. Gale, A. García, J. Junquera, D.Sànchez-Portal, R.M. Martin, SIESTA 2.0 User's guide, available: http://www.uam.es/siesta.

[11] J. Junquera, Ó. Paz, D.Sànchez-Portal, E. Artacho, Phys. Rev. B 64, 235111, (2001).

[12] LCAO approach, available: http://phycomp.technion.ac.il/ anastasy/teza/teza/node17.html.

[13] Linear Combination of Atomic Orbitals (LCAO), available: http://users.aber.ac.uk/ruw/teach/235/lcao.html.

[14] R.M Martin, Electronic Structure (Basic Theory and Practical Methods), Cambridge University Press, (2004).

[15] A. Groß, Theoretical Surface Science, Springer, (2003).

[16] W.Kohn, L.J. Sham, Phys. Rev. 140, 1133, (1965).

[17] D.Vanderbilt, Phys. Rev. B 41, 7892, (1990).

[18] P. E. Blöchl, Phys. Rev. B 50, 17953, (1994).

[19] Valentin, C.D., Figini, A., Pacchioni, G., Surf. Sci. 556, 145, (2004).

[20] Lee, J., Lee, J.-G., Yates, J. T., Surf. Sci. 594, 20, (2005).

[21] Gee, A.T., Hayden, B.E., J. Chem. Phys. 113, 10333, (2000).

[22] A. Puisto, Oxygen adsorption on clean and oxygen precovered Cu(100), Master's Thesis, Lappeenranta University of Technology, (2003).

[23] A. Groß, Dissociative adsorption of Hydrogen on Pd(100), available: http://www.fhi-berlin.mpg.de/th/Highlights.

[24] J. Behler, B. Delley, S. Lorenz, K. Reuter, M. Scheffler, Phys. Rev. Let.94, 036104, (2005).

[25] D.A Kofke, Molecular simulation course material, available: http://www.cheme.buffalo.edu/courses/ce530/.

[26] S. Nosé, J. Chem. Phys. 81, 511, (1984).

[27] S. Nosé, Mol. Phys. 52, 255, (1984).

[28] D.M. Lind, F.B. Dunning, G.K Walters, Phys. Rev. B 35, 9037, (1987).

[29] A. Puisto, M. Alatalo, A.S. Foster, K. Laasonen, unpublished.

[30] H. J. Monkhorst and J. D. Pack, Phys. Rev. B 13, 5188, (1976).

[31] N. Nivalainen, Adsorption of atomic oxygen on Ag/Cu(100), Electronics project work, 2004, unpublished.

[32] C. Kittel: Introduction to Solid State Physics, John Wiley & Sons Inc., (1971).

[33] P. Junell, M. Ahonen, M. Hirsimäki, M. Valden, Surf. Rev. Lett. 11, 457, (2004).

[34] M. Lampimäki et al: Surface oxidation of Cu(100), Cu(Ag) and OFHC-Cu Studied by XPS and TEM, poster, (2004).

[35] M. Hirsimäki et al: Influence of Adsorbate induced segregation of copper on the surface oxidation of copper-siler alloys, poster, (2005).

[36] M. Hirsimäki, M. Lampimäki, K. Lahtonen, I. Chorkendorff, M. Valden, Surf. Sci., 583, 157, (2005).

[37] O.M Løvvik, Surf. Sci. 583, 100, (2005).

[38] E. Christoffersen, P. Stoltze, J.K. Nørskov, Surf. Sci. 505, 200, (2002).

[39] J. Nerlov, I. Chorkendorff, J. of Catal. 181, 271, (1999).

[40] T. Kangas, K. Laasonen, A. Puisto, H. Pitkänen, M. Alatalo, Surf. Sci. 584, 62, (2005).

[41] M. Gajdoŝ, A. Eichler, J. Hafner, Surf. Sci., 531, 272, (2003).

[42] T. Kangas, N. Nivalainen, H. Pitkänen, A. Puisto, M. Alatalo, K. Laasonen, Surf. Sci. 600, 4103, (2005).

[43] Y. Xu, M. Mavrikakis, Surf. Sci. 538, 219, (2003).

[44] H. Le Rouzo, P. Parneix, G. Raseev, K.S. Smirnov, Surf. Sci. 415, 131, (1998).

[45] M.-C. Marinica, G. Raşeev, Surf. Sci. 497, 227, (2002).

[46] M.-C. Marinica, H. Le Rouzo, G. Raşeev, Surf. Sci. 542, 1, (2003).

[47] M. Gajdoš, A. Eichler, J. Hafner, G. Meyer, K.H. Rieder, Phys. Rev. B 71, 35402, (2005).

[48] J. Braun, A.P. Graham, F. Hofmann, W. Silvestri, J. Toennies, G. Witte, Journal of Chem. Phys. 105, 3258, (1996).

[49] S. Fölsch, A. Helms, A. Riemann, The Free University of Berlin, Institution of experimental physics, available: http://www.physik.fu-berlin.de/ ag-rieder/smoke.html.

[50] M. Lahti, Poisoning effect of S on Pd surfaces, Master's Thesis, Lappeenranta University of Technology, (2005).

[51] Center for Atomic-scale Materials Physics of Technical University of Denmark, available: http://dcwww.camp.dtu.dk/campos//Dacapo/manual/manual.html.

[52] J.K. Nørskov, T. Bligaard, A. Logadottir, S. Bahn, L.B. Hansen, M. Bollinger, H. Bengaard, B. Hammer, Z. Slijivancanin, M. Mavrikakis, Y. Xu, S. Dahl, C.J.H. Jacobsen, Journ. of Catal. 209, 275, (2002).

[53] Xu, Y., Mavrikakis, M., Surf. Sci. 494, 131, (2001).